

Load-Dependent Active Thermal Control of Grid Forming Converters

Markus Andresen, *Member, IEEE*, Giovanni De Carne, *Member, IEEE* and Marco Liserre, *Fellow, IEEE*

Abstract—Grid forming converters enable an asynchronous connection of grids, which opens new opportunities for the power system management. This includes the potential to control the amplitude and the frequency of the grid voltage to vary the power consumption of the loads and the generation in the grid. Depending on the load sensitivity to voltage and frequency, the power transfer of the grid forming converter changes. Remarkably, this has an impact on the power semiconductors by means of thermal stress, which is limiting the lifetime of the devices. This work aims to investigate and mitigate the thermal stress in grid-forming converters by applying a load voltage-sensitivity control. Depending on the nature of the loads, their power consumption varies with the voltage. This response is dependent on the connected loads and can be characterized by constant power (independent from the voltage), constant current (linearly dependent on the voltage) and constant impedance behavior (squared-dependent on the voltage). The sensitivity to voltage is exploited to control the load power consumption, reducing the junction temperature fluctuations and thus the power semiconductors stress.

Index Terms—Power Electronics, Reliability, Power system control, Temperature control, DC-AC power conversion

I. INTRODUCTION

The power volatility introduced by renewables calls for a fast and reliable control of power grids. For improving the grid management, the asynchronous connection of grids represent a viable solution [1], which allows the independent control of connected grids by decoupling the grid's AC power flow. Several applications of asynchronously grids are mentioned at different voltage levels, such as High Voltage Direct Current (HVDC) systems in High Voltage (HV) grids [2]. These systems, transferring power between remote points of the grid, have demonstrated technical and economical advantages in applications such as on-shore and off-shore wind power plant connection [3], [4]. In Medium Voltage (MV) and Low

Voltage (LV) grids, asynchronous connections, such as Smart Transformers (ST) [5], can control the grid by shaping the consumption of voltage-dependent loads varying the voltage, and thus operating like a controllable resource [6]. The secondary side of an asynchronous connection is typically controlled in grid-forming mode, that implies a direct control of the voltage waveform in the fed grid. As consequence, the power processed by the converter cannot be controlled directly, but it depends solely on the load power demand [7]. In particular conditions of high power demand, the power semiconductor's in the converter can suffer from high thermal stress, that is further worsened by intermittent power fluctuations. To reduce the thermal stress for the semiconductors, the grid forming converter can exploit its voltage control feature to shape the load consumption in controlled way and thus to damp the power variations at grid forming converter level [8]–[10]. The possibility to decrease the load consumption by lowering the voltage has been already considered in the Conservation Voltage Regulation (CVR) approach for energy saving purposes [11], and in the voltage-led load management to provide demand response capability to the distribution grid without the need of a communication infrastructure [12]–[14]. The shaping of the load consumption can provide a large power reserve at practically no costs, as shown in [13], where up to 3 GW of power reserve are available in United Kingdom in case of a fast demand reduction is needed.

However, in the aforementioned applications the power (or current) reduction cannot be evaluated in advance of the control action, because the load sensitivities to voltage are not taken into account by the controller. Depending on the overall grid sensitivity to voltage, a decrease of the grid voltage can even increase the thermal stress for power semiconductors in the grid forming converter, that depends mainly on the grid current. In presence of constant power loads, a voltage reduction leads to a current increase, and thus to higher thermal stress. Consequently, knowing the load sensitivity before the control action application is fundamental for a proper grid management [8], [15].

This work is based on a previous conference article [16], which introduces the potential of controlling the grid voltage amplitude. This is done aiming at increasing the maximum operating range of the grid-forming converter by reducing the thermal stress on the power semiconductors. Acting on the voltage amplitude, and considering the voltage sensitivity as explained in [15], the thermal stress impact on the grid-forming converter can be minimized, by controlling the current demand from the converter-fed loads. The damage reduction is quantified and the obtained results are compared to the application of classical CVR schemes, where the load sensitivity

Manuscript received July 25, 2019; revised Oct 14, 2019; accepted December 2, 2019. Date of publication Dec 11, 2019; date of current version Dec 11, 2019. 2019-IACC-1027.R1, approved for publication in the Industrial Automation and Control Committee of the IEEE Industry Application Society. The work was supported in part by the European Research Council under the European Union's Seventh Framework Programme (FP/2007-2013) / ERC Grant Agreement n. [616344] - HEART, the German Federal Ministry of Education and Research (BMBF) within the Kopernikus Project ENSURE "New ENergy grid StructURes for the German Energiewende" (03SFK110), the German Federal Ministry for Economic Affairs and Energy (BMWi) within the Project KielFlex Kiel als Vorbild für die Errichtung von Ladeinfrastruktur in einem flexiblen Stromnetz zur Umsetzung einer Emissionsreduktion im Transportsektor (01MZ18002D) and by the Ministry of Science, Research and the Arts of the State of Baden-Württemberg Nr.33-7533.-30-10/67/1. (Corresponding author: Markus Andresen.)

Markus Andresen and Marco Liserre are with the Chair of Power Electronics, Christian-Albrechts Universität zu Kiel 24118 Kiel, Germany (e-mail: ma@tf.uni-kiel.de, liserre@ieee.org.)

Giovanni De Carne is with the Institute for Technical Physics, Karlsruhe Institute of Technology, Karlsruhe, Germany (e-mail: giovanni.carne@kit.edu.)

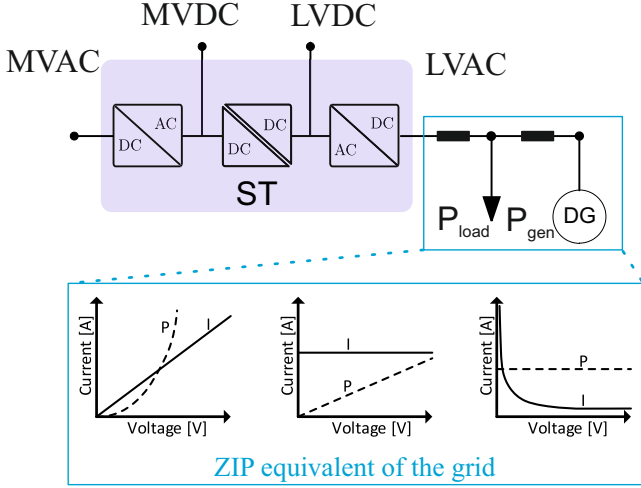


Fig. 1: Current and Power characteristics for constant impedance load (left), constant current load (centre) and constant power load (right).

to voltage is not considered.

In section II this work provides the basic concepts of the grid voltage sensitivity along with the importance of the junction temperature for the reliability of the power converter. Section III demonstrates the capability of the voltage to the stress in case of a constant impedance, constant power and constant current load. In the fourth section, experimental results are shown to validate the potential of the introduced approach and the results are concluded in section V.

II. GRID VOLTAGE SENSITIVITY AND JUNCTION TEMPERATURE MODELING

This section introduces the concept of different load sensitivity to voltage, which is resulting in different power consumption of the grid. Afterwards, the impact of power electronics based loads is discussed and the importance of the power semiconductor's junction temperature and its impact on the power semiconductors lifetime is examined.

A. Load sensitivity to grid voltage

Load composition in the distribution grid has changed significantly in the last years, due to the large integration of power electronics-based loads, such as laptops, cell phone charges, flat screen TVs, etc. [17]. The latter are practically insensitive to voltage variations, having the power electronics interface to regulate the current consumption by following the voltage. On the other hand, there are still voltage-dependent loads, such as refrigerators, compressors, and elevators, that are largely present in distribution grids [18]. Typically the load sensitivity to voltage is classified in three main categories:

- Constant impedance load (e.g. incandescent lighting, unregulated motors)
- Constant power load (e.g. converter feed variable speed drives, computer, TV)
- Constant current load (e.g. fluorescent lighting)

The load dependency on voltage can be expressed mathematically in a simplified way, by means of a exponential function:

$$P = P_0 \cdot \left(\frac{V}{V_0}\right)^{k_p} \quad (1)$$

where P is the power consumption at a certain voltage V and P_0 is the nominal power demand at reference voltage V_0 , and k_p represents the exponential parameter that characterizes the dependency of the power consumption on voltage. To introduce the fundamentals of the proposed concept, the equations for the three load sensitivity categories are listed below. In case of a constant impedance load, the power can be expressed as:

$$P = \frac{V^2}{R} = P_0 \cdot \left(\frac{V}{V_0}\right)^2 \quad \text{for constant impedance loads} \quad (2)$$

where R is the resistance of the load. The constant current load and the constant power load are expressed with the current I in (3) and (4), respectively:

$$P = V \cdot I = P_0 \cdot \left(\frac{V}{V_0}\right)^1 \quad \text{for constant current loads} \quad (3)$$

$$P = P_0 = P_0 \cdot \left(\frac{V}{V_0}\right)^0 \quad \text{for constant power loads} \quad (4)$$

To visualize the impact of the load sensitivity, an ST-fed distribution grid is shown in Fig. 1, where the aforementioned three main load sensitivity categories are conceptually represented in the same figure. A constant impedance load varies quadratically the power consumption following a voltage change, whereas a constant current load varies the power linearly with the voltage, leaving the current unchanged. In case of a constant power load, the power is independent from the voltage level, whereas the current is inversely proportional to the voltage.

Remarkably, a variation of the voltage has a different impact on the power consumption of the load. In particular for the constant impedance load case, an increase of the grid voltage has an opposite effect than for the constant power load. For this reason, knowledge about the load sensitivity is of high importance, if the grid voltage wants to be used as control variable for minimizing the power semiconductor's stress.

It is important to highlight that the distributed generation in the grid can influence the sensitivity of the grid net load (load-generation) as well. As demonstrated in [8], the active power injection of the generation is independent from the voltage amplitude. Feeding constant power into the grid during a voltage variation, the generation makes the grid net load more sensitive to voltage variations, as in can be interpreted from (5):

$$P(V) = P_0 \cdot \left(\frac{V}{V_0}\right)^{k_p \cdot \frac{P_{load}}{P_{load} - P_{gen}}} \quad (5)$$

where P_{load} is the load demand and P_{gen} is the active power produced by the generators. As can be noted, an

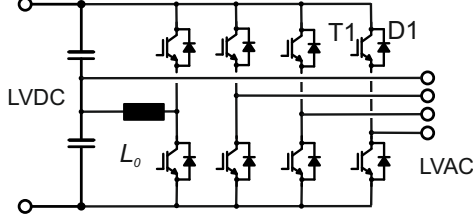


Fig. 2: Two level voltage source converter.

increasing power production P_{gen} , under constant load consumption conditions, increases voltage sensitivity of the net load in the grid ($P_{load} - P_{gen}$), despite an unchanged net-load consumption. The dependency of the net-load sensitivity gives strong argumentation in evaluating the load sensitivity in real-time or in short intervals [15].

B. Load dependency on voltage in distribution grids

Since this work aims to reduce the thermal stress in grid-forming converters, a discuss on the current load dependency on voltage in distribution grids is necessary to address properly the control strategy. As already mentioned in the introduction, power electronics-based appliances, largely present in LV grids, are mostly insensitive to voltage, in order to maximize the power quality and increase the efficiency at the load side. On the other hand, there is still a large amount of voltage-dependent loads in the grid. To this category belong the air conditioner, induction lights, microwaves and refrigerators, that have a consistent constant impedance contribution in the power absorption, as shown in [18]. If these loads are aggregated in a residential grid together with constant power loads, the aggregate load is still sensitive to voltage variations, resulting in $k_p < 1$ pu [18]. In the field experiments carried out in [19], the Serbian distribution grid showed a high sensitivity to voltage variations $k_p = [1.1...1.4]$ pu. More recent field results show similar findings [13], with the UK distribution grid behaving as constant current load (i.e., $k_p \approx 1$), making available a reasonable margin for voltage-based control actions. From the results mentioned above, the load shows still a voltage-dependent behavior, that can be employed for corrective voltage-based control actions in the distribution grid.

C. Thermal stress and junction temperature modeling

The wear out and failure mechanisms of power semiconductors are caused by thermal stress, which affects the interfaces between layers of materials with different coefficients of thermal excursion. During operation, the mission profile causes power variations, creating losses variation and therefore varying junction temperature. As result, the wear-out and potentially a failure of the device are possible, where the most commonly found failure mechanisms are bond wire liftoff and solder fatigue [20].

A common way to express the lifetime of a power semiconductor is schematically expressed in (6), where the lifetime of semiconductors is quantified by the manufacturer in

dependence of the number of junction temperature swings N_f with the magnitude ΔT_j and the average junction temperature $T_{j,av}$ with the fitting parameters a_1, a_2 and a_3 . Remarkably, the magnitude of the junction temperature has exponential influence on the lifetime of the devices.

$$N_f = a_1 \cdot (\Delta T_j)^{a_2} e^{\frac{a_3}{T_{j,av}}} \quad (6)$$

For the evaluation of the lifetime, the damage is commonly accumulated linearly with Miner's rule shown in (7)

$$C = \sum_i \frac{n_i}{N_i} \quad (7)$$

Here C is the cumulative damage, n_i the number of cycles in the stress range i and N_i the number of cycles to failure in the i -th stress range. Thus, the more thermal cycles occur in the mission profiles the more the cumulative damage will rise. If the cumulative damage reaches 1, the module will fail according to the model [21].

As a consequence, the reduction of junction temperature fluctuations for increasing the lifetime of the power semiconductors is targeted. Such strategy, implemented by means of software, is normally referred as active thermal control [22] and, in the following, it is performed assuming the grid voltage as control variable.

III. IMPACT OF GRID VOLTAGE VARIATION ON JUNCTION TEMPERATURE

The operative conditions of power converters have an impact on its reliability [23], [24]. This section investigates how the grid voltage control can be used to reduce thermal stress for the power semiconductors in a power converter. Therefore, the losses of the converter need to be derived for different voltage-dependent load types. Without losing in the converter topology generality, this work adopts a two level voltage source converter in the analysis, as shown in Fig. 2. For obtaining the junction temperatures of the semiconductors, the switching losses and the conduction losses are derived for switching devices and diodes, respectively. For the switches, Insulated Gate Bipolar Transistors (IGBT)s are considered and the switching losses $P_{sw,T}$ and the conduction losses $P_{cond,T}$ can be derived with (8) and (9) respectively [25].

$$P_{sw,T} = f_{sw} \cdot E_{sw} \frac{\sqrt{2}}{\pi} \cdot \frac{I}{I_{ref}} \cdot \left(\frac{V}{V_{ref}}\right)^{1.3} (1 + C_{sw}(T_j - T_{ref})) \quad (8)$$

$$P_{cond,T} = \left(\frac{1}{2\pi} + \frac{m \cdot \cos \varphi}{8}\right) v_{ce,0}(T_j) \cdot I + \left(\frac{1}{8} + \frac{m \cdot \cos \varphi}{3\pi}\right) r_{ce}(T_j) \cdot I^2 \quad (9)$$

In this equation f_{sw} is the switching frequency, m the modulation index, $\cos(\varphi)$ the power factor, C_{sw} is a parameter showing the temperature dependence of the losses and E_{sw} is the sum of the turn-on and turn-off losses at the reference current I_{ref} , the reference voltage V_{ref} and the reference temperature T_{ref} . The conduction losses are approximated with the temperature dependent voltage drop $v_{ce,0}$ and the resistance r_{ce} . In a similar way, the conduction losses of the diodes

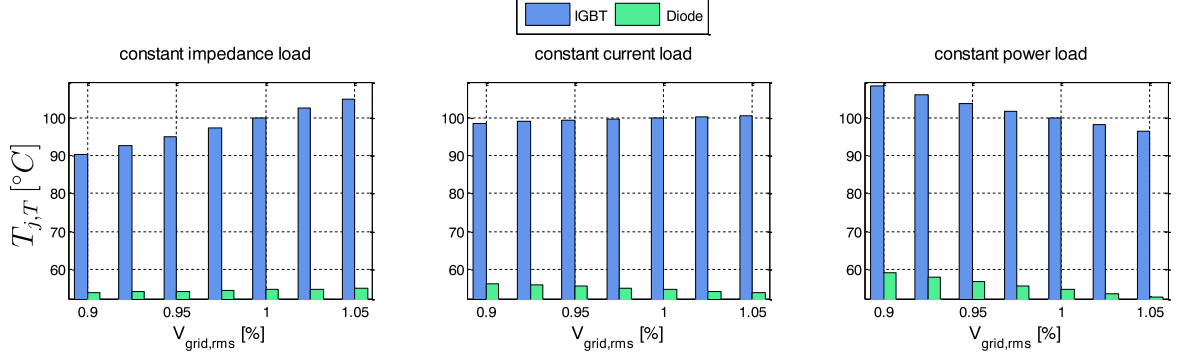


Fig. 3: Junction temperatures of IGBT and diode for varying grid voltage $V_{grid,rms}$ and different load types. No distributed generation.

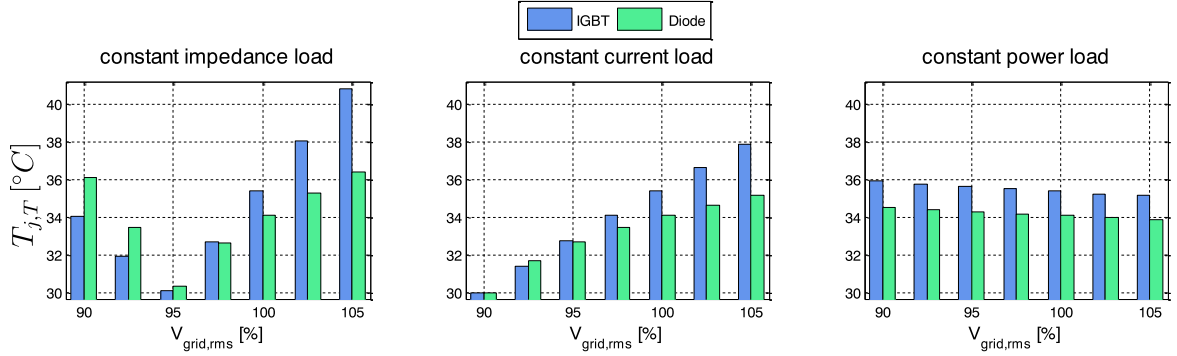


Fig. 4: Junction temperatures of IGBT and diode for varying grid voltage $V_{grid,rms}$ and different load types. 90% distributed generation.

$P_{cond,D}$ and the reverse recovery losses P_{rr} can be expressed with (10) and (11).

$$P_{rr} = f_{sw} \cdot E_{rr} \frac{\sqrt{2}}{\pi} \cdot \frac{I}{I_{ref}} \cdot \left(\frac{V}{V_{ref}}\right)^{1.3} (1 + C_{SW}(T_j - T_{ref})) \quad (10)$$

$$P_{cond,T} = \left(\frac{1}{2\pi} + \frac{m \cdot \cos \varphi}{8}\right) v_{d,0}(T_j) \cdot I + \left(\frac{1}{8} + \frac{m \cdot \cos \varphi}{3\pi}\right) r_d(T_j) \cdot I^2 \quad (11)$$

In these equations, E_{rr} represents the reverse recovery losses, $v_{d,0}$ is the on state voltage drop of the diode and r_d is the resistance of the diode. For obtaining the junction temperature in stationary conditions $T_{j,T}$, the losses of the transistors can be multiplied with the thermal resistance between junction and case $R_{th,jc}$ and need to be added to the case temperature T_c . This is shown for the junction temperature of the IGBT in (12), where the conduction and switching losses of the IGBT are considered.

$$T_{j,T} = T_c + R_{th,jc} \cdot (P_{cond,T} + P_{sw,T}) \quad (12)$$

This equation only holds for stationary analysis. However, it is used in the following to evaluate the potential of the grid voltage variation for the thermal stress reduction of the semiconductors. The effect of varying the grid voltage on the junction temperature of the devices in the interval $V_{grid,rms} = [0.9 \dots 1.05]$ pu is demonstrated for the three different load types without additional distributed generation in the grid

in Fig. 3. As expected, it can be seen that the losses can be influenced and therefore the junction temperature. In case of the constant impedance load, the junction temperatures of both devices increase with increasing grid voltage. For the constant current load, the variation of the voltage has only a minor effect on the junction temperatures and the constant power load shows reduced junction temperatures for increasing grid voltage. Remarkably, the knowledge of the load behavior is important for determining the correct control action in the voltage control. The highest potential exists for the constant impedance load, whereas the constant current load has the lowest potential.

As discussed in the theoretical analysis of section II A, the presence of distributed generation can increase the sensitivity of the load to voltage. This is shown in Fig. 4, where high penetration of renewable energy sources is considered ($P_{gen} = 0.9 P_{load}$). As it can be seen in the figure, this increases the capability to control the losses and therefore the junction temperature significantly. Here, the normed losses can be varied in a much higher range, even if the overall losses are lower than in the case before. For the constant impedance load, an overall minimum of the losses can be seen at $V_{grid,rms} = 0.95$ pu, which represents the case that the active power is generated and consumed in the ST-fed grid. For higher voltages, the power needs to be injected, whereas it needs to be absorbed by in case of lower voltages. Similarly, for the constant current load, the minimum of the junction

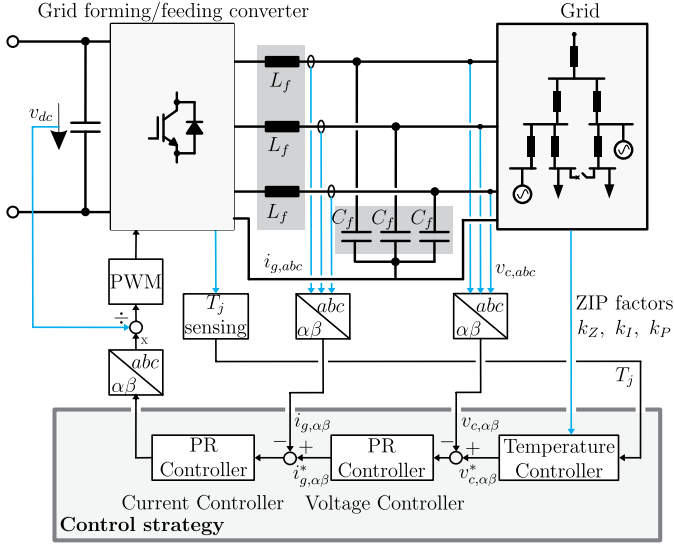


Fig. 5: Scheme of the proposed grid forming control with additional temperature control loop.

temperature is at $V_{grid,rms} = 0,9 pu$, because this represents equal load and generation in the grids. For the constant power loads, the junction temperatures shows a low sensitivity to voltage for the investigated grid voltage range by a maximum junction temperature difference of $1K$.

IV. REDUCTION OF THE JUNCTION TEMPERATURE FLUCTUATIONS

In this section the thermal controller design is demonstrated and an evaluation of the junction temperature for the most extreme load cases is shown.

A. Temperature controller design

For the goal of the thermal stress reduction, the junction temperature is proposed to be controlled by controlling the grid voltage. This is done in an additional cascaded loop as shown in Fig. 5. The junction temperatures of the power semiconductors are sensed as well as the load sensitivity for setting the reference voltage of the grid. With this information, the grid voltage is controlled with two cascaded Proportional Resonant (PR) controllers.

The temperature controller is implemented with a Proportional Integral (PI) controller and the open loop transfer function of the system $G_{th,ol}(s)$ is expressed with:

$$G_{th,ol}(s) = \frac{T_j \cdot T(s)}{V(s)} = G_V(s) \cdot G_{th}(s) \cdot G_{loss}(s) \cdot G_{PI}(s) \quad (13)$$

In this equation, $G_V(s)$ is the closed loop voltage controller, $G_{th}(s) = Z_{th,jc}(s)$ is the thermal impedance of the power module, G_{loss} is the transfer function between losses and grid voltage and $G_{PI}(s)$ is the transfer function of the PI-controller. As it can be seen in (8) and (9), the transfer function between the grid voltage and the power semiconductor losses is partially independent from the voltage and partially non-linear. However, due to the small variation of the grid voltage, it is

approximated with $G_{loss} = k_{loss}$. Remarkably, the temperature controller is designed with an inner voltage controller. This limits the potential bandwidth of the junction temperature controller and results in the challenge to cope with the small time constants of the thermal impedance.

In the following, a single thermal chain is considered for G_{th} in (13) and is used to derive the open loop transfer function. Therefore, the PI-controller is tuned with the technical optimum, resulting in the cancellation of the zero of the PI-controller with the pole of the thermal impedance. This results in:

$$G_{th,ol}(s) = \frac{K_{PI} \cdot R_{th,eq} \cdot k_{loss}}{T_i s + T_i T_d s^2} \quad (14)$$

In this equation, $R_{th,eq}$ is equivalent thermal resistance of the first order thermal chain, T_i is the time constant of the integrator, K_{PI} is the proportional gain of the integrator and T_d represents the equivalent time constant of the voltage control loop. As a result, the closed loop can be expressed with:

$$G_{th,cl}(s) = \frac{1}{1 + \frac{T_i}{K_{PI} \cdot R_{th,eq} \cdot k_{loss}} s + \frac{T_i T_d}{K_{PI} \cdot R_{th,eq} \cdot k_{loss}} s^2} \quad (15)$$

This equation needs to be evaluated carefully, because the thermal model is only evaluated for a single thermal chain. It results in the negligence of the fast thermal dynamics (at the junction) and the slow thermal dynamics (of the cooling system). Consequently, the parameters of the PI-controller may need to be adjusted to obtain good dynamic performance.

B. Evaluation of the impact of grid voltage control on the thermal stress

For evaluating the performance of the thermal controller, a mission profile for a grid with fast changing power cycles is considered. The profile length is chosen to be one minute in order to obtain a time period in which reasonable fast power variations occur, which can still be simulated. The applied thermal model is described in [26] and it is suitable for enabling thermal simulations with relatively long time periods of several minutes. The considered mission profile is simulated for the two most extreme load behaviors with respect to the grid voltage sensitivity, which are the constant impedance load and the constant power load. Any other mix of the load composition, assuming no distributed generation, will have a lower grid voltage sensitivity. For the investigation of the junction temperature sensitivity to the load composition, the junction temperature is simulated for the case with constant nominal grid voltage, the application of CVR ($0.95 V_0$) and the temperature control. The thermal profiles for the case of a constant impedance load are shown in Fig. 6.

In the figure, only a moving average of the junction temperature $T_{j,mean}$ is shown, because otherwise the junction temperature cycles affected by the fundamental frequency of the grid ($f_g = 50Hz$) are visually dominant. As it can be seen in the figure, the junction temperature follows the current profile, as expected. The CVR achieves a reduction of the load current and therefore of the temperature. The temperature control instead is acting like CVR for roughly half of the time

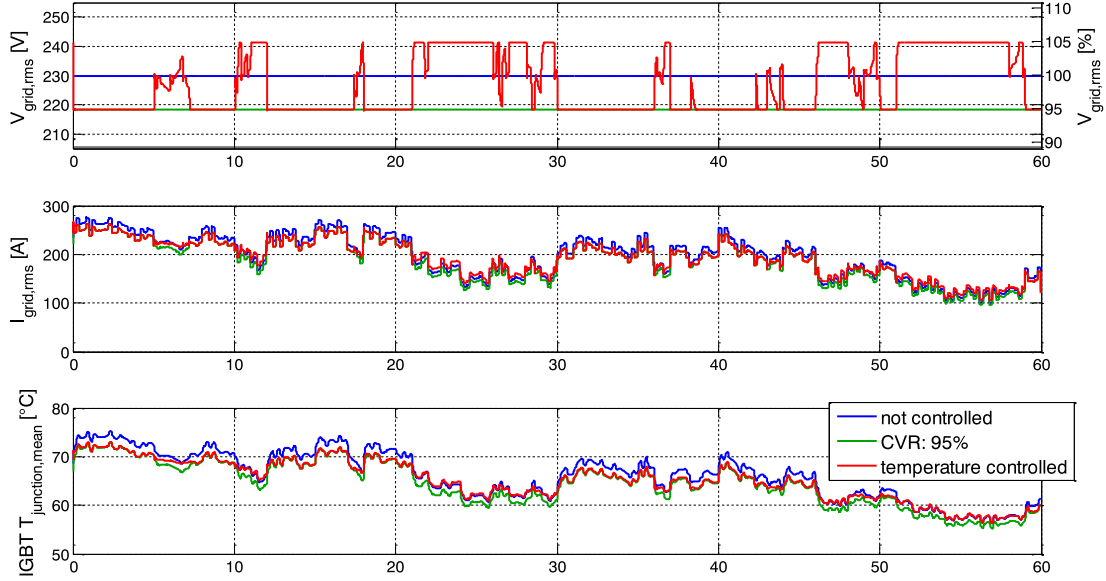


Fig. 6: Simulated junction temperature of an IGBT in the 2 level voltage source converter feeding a constant impedance load based grid for a mission profile with fast changes in the power consumption and generation. Comparison between operation with constant voltage, CVR (grid voltage = 95% of nominal grid voltage) and junction temperature control.

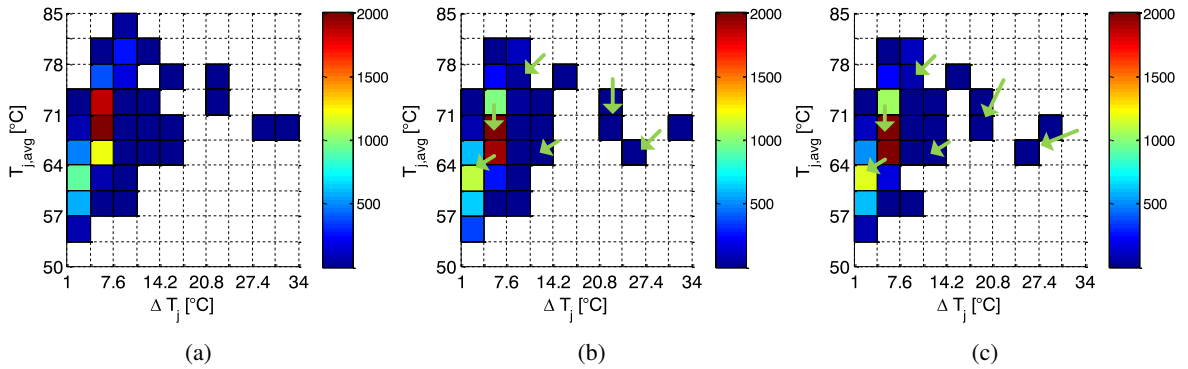


Fig. 7: Rainflow counted thermal cycles of the voltage control strategies of the converter feeding a constant impedance load as shown in Fig. 6: (a) Constant nominal grid voltage, (b) CVR, and (c) temperature control.

	Normalized damage	Damage reduction (CVR)	Damage reduction (temperature control)
Const. Z-load	100 %	40.4 %	42.7 %
Const. P-load	100 %	31.3 %	33.1 %

TABLE I: Reduction of the accumulate damage for the constant impedance load (Const. Z-load) and the constant power load (Const. P-load) for the simulations with constant grid voltage, application of CVS and temperature control.

Symbol	Description	Value
V_0 (rms)	Grid voltage (rms)	120V
f_g (rms)	Grid frequency	50Hz
L_g	Filter inductance	3.5mH
V_{DC}	DC-link voltage reference	400V
P_{load}	Load power	5kW
P_{gen}	Power of distributed generation	0kW
$[k_z; k_I; k_P]$	ZIP composition	[1;0;0]

TABLE II: Parameters of the experimental setup.

and increases the voltage to increase the temperature during down swings of the load power demand of the grid. The related junction temperature is lower than the one of the constant voltage case and higher than the one of the CVR case.

For the evaluation of the thermal stress, Rainflow counting is applied to count the thermal cycles of the temperature profile. This is shown for the junction temperature profile of the constant impedance load under the application of the three control strategies in Fig. 7. As it can be seen, the thermal cycles are shifted to lower temperature magnitudes $T_{j,avg}$ and

to lower thermal swings ΔT_j . Remarkably, the influence of the CVR and the temperature control is comparable.

The same mission profile is run for a constant power load. In this case, the results of the Rainflow counting for the junction temperature profile of the IGBT is shown in Fig. 8. Similar to the constant impedance load, the CVR and the temperature control achieve a very similar shift of the mean temperature $T_{j,avg}$ of the thermal cycles and their magnitude T .

For the evaluation of the lifetime impact of the proposed method, Miner's rule (7) is applied for the constant impedance

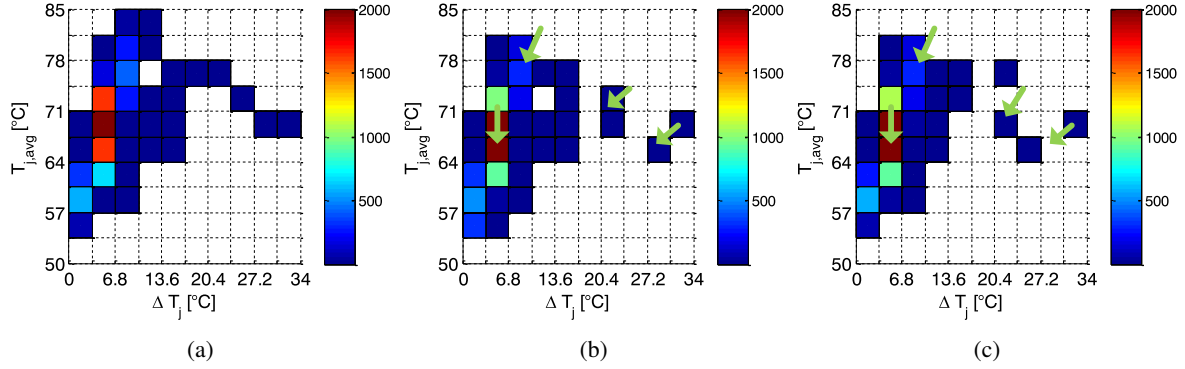


Fig. 8: Rainflow counted thermal cycles of the voltage control strategies of the converter feeding a constant power load: (a) Constant nominal grid voltage, (b) CVR, and (c) temperature control.

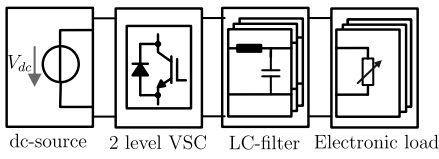


Fig. 9: Scheme of the test bench used to obtain the experimental results.

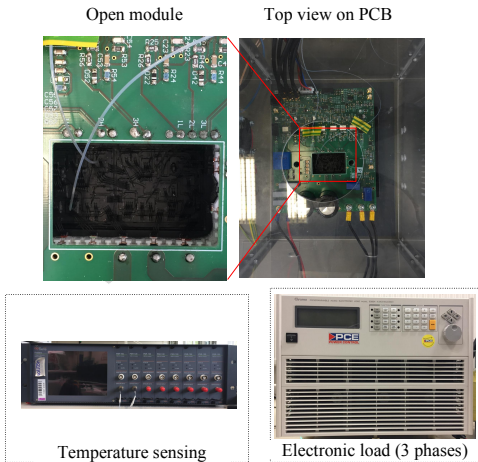


Fig. 10: Picture of the power converter, the junction temperature sensing system and the electronic load.

load case and the constant power load case in with the CVR and the junction temperature control strategy. The results of the damage evaluation is normalized and shown in Table I. As it can be seen, the thermal stress reduction by applying the CVR is 40% in case of a constant impedance load and 31% for a constant power load, respectively. The difference compared to the active temperature control achieves in both cases an additional damage reduction of 2%. This value is superior to the CVR, and simultaneously, more energy is supplied to the loads. In contrast to CVR, the proposed control manipulates the losses and thereby the thermal stress for the devices in the ST.

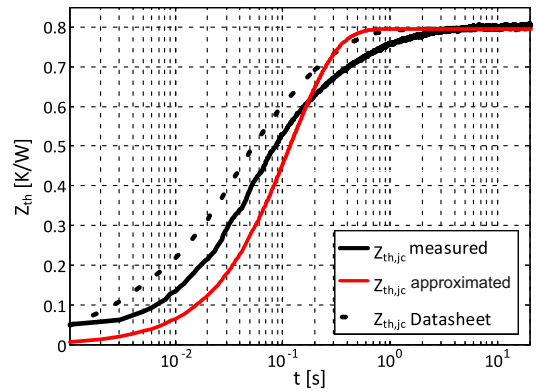


Fig. 11: Thermal impedance of the power electronic module between junction and case $Z_{th,jc}$, approximation to a single order function and thermal impedance of the datasheet.

V. EXPERIMENTAL VALIDATION

To validate the effectiveness of the proposed method, an experimental setup consisting of a 2 level voltage source converter is built, which feeds a load in grid-forming operation. The grid is emulated by a three-phase electronic load and a scheme of the overall setup is shown in Fig. 9. The parameters of the setup are provided in Table II and the most relevant parts of the setup are shown in Fig. 10. The junction temperature of the power semiconductors in the converter are directly measured with an Opsens ProSens system, enabling sensor response times of 5 ms. The thermal impedance of the adopted power electronic module is characterized experimentally and fit to a single order transfer function with a least mean square algorithm. The measured temperature is compared to the value from the datasheet as shown in Fig. 11. As it can be seen, there is a significant deviation between the thermal impedance provided in the datasheet and the thermal impedance of the measurement, whereas the thermal resistance is similar for both cases. Therefore, to use the correct dynamics of the temperature controller, it is advised to characterize the device before implementing the controller. In this case, the first order of the thermal impedance obtains a time constant of ($\tau = 0.2$ s) and an $R_{th,jc} = 0.8$ K/W.

Similar to the simulation study, three different voltage con-

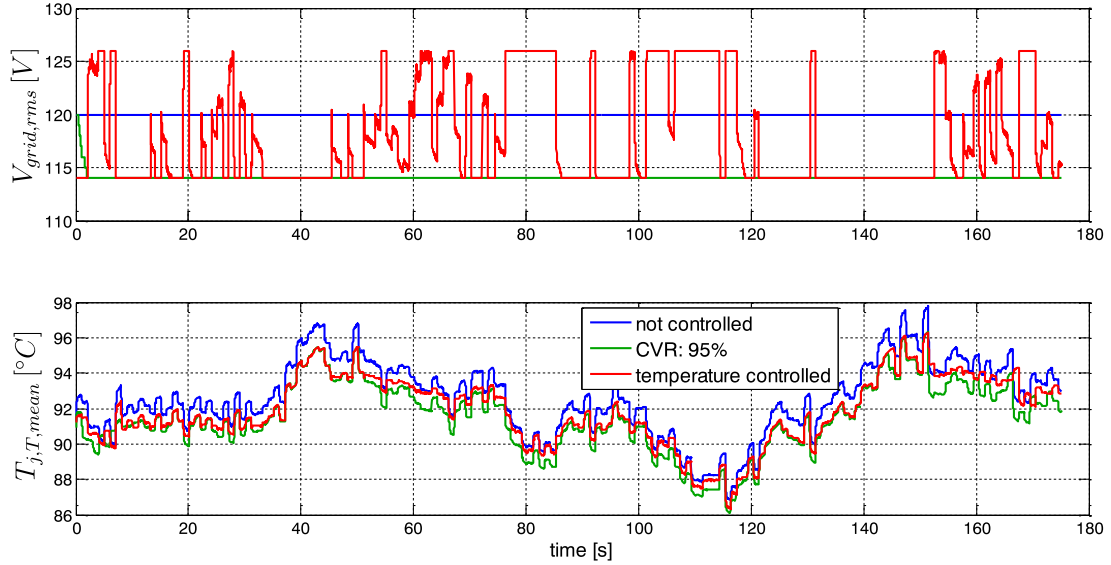


Fig. 12: Measured junction temperature of an IGBT in the 2 level voltage source converter feeding a constant impedance load based grid for a mission profile with fast changes in the power consumption and generation. Comparison between operation with constant voltage, CVR (grid voltage = 95% of nominal grid voltage) and junction temperature control.

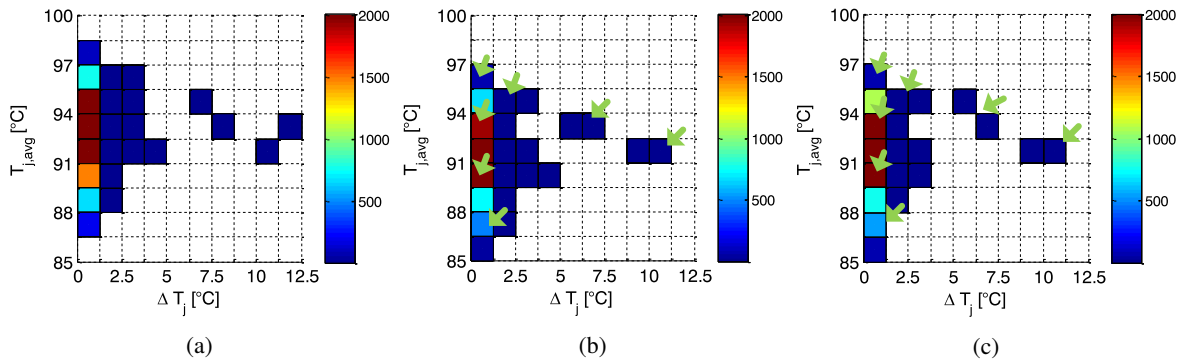


Fig. 13: Experimental measurement of the Rainflow counted thermal cycles in a grid forming converter feeding a constant impedance based grid as shown in Fig. 12: (a) Constant nominal grid voltage, (b) CVR, and (c) temperature control.

control strategies are tested, which is shown in Fig. 12. The first case shows the junction temperature undergoing a profile with constant nominal voltage, the second case shows the junction temperature for the application of CVR and the third case applies directly the junction temperature control. In the case with constant voltages, the junction temperature profiles obtain a similar characteristic behavior and the reduced voltage results, as expected, in a reduced junction temperature. The proposed junction temperature control affects a dynamical variation of the voltage. Consequently, the junction temperature of the power semiconductor is always higher than the temperature in the case when CVR is applied. Rainflow counting is applied for visualizing the laboratory results and for highlighting the impact of the voltage control strategies on the thermal cycles, which is shown in Fig. 13.

In Fig. 13 (a) the result with constant nominal voltage is shown. Remarkably, most identified thermal cycles are $\Delta T_j < 5 K$ and some further thermal cycles can be seen. For the application of CVR and the junction temperature control, the thermal cycles are reduced in magnitude and in the number,

which is highlighted with arrows in Fig. 13 (b) and (c).

The results of the laboratory experiment in terms of accumulated damage are also similar to the simulation results. However, for the comparison of the different strategies, the accumulated damage is derived as benchmark to evaluate the effectiveness of the strategies. The accumulated damage is normalized to the damage with constant rated voltage and the temperature controller achieves a reduction by 42.2%, whereas the result of CVR is 34.8% and therefore slightly lower. Therefore, the experimental results match with the results obtained in the simulations, even if the temperature control is shown to be more effective than estimated.

VI. CONCLUSION

High power injection volatility increases the thermal stress for power semiconductors in grid-forming converters. Additionally, grid voltage variations may also cause thermal stress and thereby reduce the lifetime of the devices. The potential to reduce the power semiconductors' thermal stress by means of controlling the output voltage of the grid-forming converter

has been demonstrated in this work. Therefore, the proposed strategy takes into account the load sensitivity to voltage. In comparison with existing strategies for the manipulation of the load consumption, such as the CVR, the proposed method has shown better performance. For the CVR approach, a damage reduction of 34,8 % has been evaluated, whereas the proposed active thermal control achieved a superior damage reduction of 42,2%.

ACKNOWLEDGMENT

The authors thank Mike Schloh for support of the support of the work.

REFERENCES

- [1] R. Abe, H. Taoka, and D. McQuilkin, "Digital grid: Communicative electrical grids of the future," *IEEE Transactions on Smart Grid*, vol. 2, no. 2, pp. 399–410, June 2011.
- [2] M. Guan and Z. Xu, "Modeling and control of a modular multilevel converter-based hvdc system under unbalanced grid conditions," *IEEE Transactions on Power Electronics*, vol. 27, no. 12, pp. 4858–4867, Dec 2012.
- [3] C. Meyer, M. Hoing, A. Peterson, and R. W. D. Doncker, "Control and design of dc grids for offshore wind farms," *IEEE Transactions on Industry Applications*, vol. 43, no. 6, pp. 1475–1482, Nov 2007.
- [4] C. Chou, Y. Wu, G. Han, and C. Lee, "Comparative evaluation of the hvdc and hvac links integrated in a large offshore wind farm - an actual case study in taiwan," *IEEE Transactions on Industry Applications*, vol. 48, no. 5, pp. 1639–1648, Sep. 2012.
- [5] M. Liserre, G. Buticchi, M. Andresen, G. D. Carne, L. Costa, and Z. Zou, "The smart transformer: impact on the electric grid and technology challenges," *IEEE Transactions on Industrial Electronics Magazine*, June 2016.
- [6] G. D. Carne, M. Liserre, B. Xie, C. Zhong, S. A. P. Meliopoulos, and C. Vournas, "Multiphysics modelling of asynchronously-connected grids," in *2018 Power Systems Computation Conference (PSCC)*, June 2018, pp. 1–8.
- [7] J. Rocabert, A. Luna, F. Blaabjerg, and P. Rodríguez, "Control of power converters in ac microgrids," *IEEE Transactions on Power Electronics*, vol. 27, no. 11, pp. 4734–4749, Nov 2012.
- [8] G. De Carne, G. Buticchi, M. Liserre, and C. Vournas, "Load control using sensitivity identification by means of smart transformer," *IEEE Transactions on Smart Grid*, vol. PP, no. 99, pp. 1–1, 2017.
- [9] G. De Carne, G. Buticchi, M. Liserre, and C. Vournas, "Real-time primary frequency regulation using load power control by smart transformers," *IEEE Transactions on Smart Grid*, vol. 10, no. 5, pp. 5630–5639, Sep. 2019.
- [10] A. Ciocia, V. A. Boicea, G. Chicco, P. Di Leo, A. Mazza, E. Pons, F. Spertino, and N. Hadj-Said, "Voltage control in low-voltage grids using distributed photovoltaic converters and centralized devices," *IEEE Transactions on Industry Applications*, vol. 55, no. 1, pp. 225–237, Jan 2019.
- [11] W. Ellens, A. Berry, and S. West, "A quantification of the energy savings by conservation voltage reduction," in *2012 IEEE International Conference on Power System Technology (POWERCON)*, Oct 2012, pp. 1–6.
- [12] A. Ballanti, L. N. Ochoa, K. Bailey, and S. Cox, "Unlocking new sources of flexibility: Class: The world's largest voltage-led load-management project," *IEEE Power and Energy Magazine*, vol. 15, no. 3, pp. 52–63, May 2017.
- [13] A. Ballanti and L. F. Ochoa, "Voltage-led load management in whole distribution networks," *IEEE Transactions on Power Systems*, vol. 33, no. 2, pp. 1544–1554, March 2018.
- [14] P. K. Sen and K. H. Lee, "Conservation voltage reduction technique: An application guideline for smarter grid," *IEEE Transactions on Industry Applications*, vol. 52, no. 3, pp. 2122–2128, May 2016.
- [15] G. De Carne, M. Liserre, and C. Vournas, "On-line load sensitivity identification in lv distribution grids," *IEEE Transactions on Power Systems*, vol. 32, no. 2, pp. 1570–1571, March 2017.
- [16] M. Andresen, G. De Carne, M. Schloh, and M. Liserre, "Active thermal control of asynchronously-connected grids considering load sensitivity to voltage," in *2018 IEEE Energy Conversion Congress and Exposition (ECCE)*, Sep. 2018, pp. 4070–4077.
- [17] K. P. Schneider, J. C. Fuller, and D. P. Chassin, "Multi-state load models for distribution system analysis," *IEEE Transactions on Power Systems*, vol. 26, no. 4, pp. 2425–2433, Nov 2011.
- [18] A. Bokhari, A. Alkan, R. Dogan, M. Diaz-Aguiló, F. de León, D. Czarkowski, Z. Zabar, L. Birenbaum, A. Noel, and R. E. Uosef, "Experimental determination of the zip coefficients for modern residential, commercial, and industrial loads," *IEEE Transactions on Power Delivery*, vol. 29, no. 3, pp. 1372–1381, June 2014.
- [19] L. M. Korunovic, D. P. Stojanovic, and J. V. Milanovic, "Identification of static load characteristics based on measurements in medium-voltage distribution network," *IET Generation, Transmission Distribution*, vol. 2, no. 2, pp. 227–234, March 2008.
- [20] M. Ciappa, "Selected failure mechanisms of modern power modules," *Microelectronics reliability*, vol. 42, no. 4, pp. 653–667, 2002.
- [21] H. Lu, T. Tilford, and D. Newcombe, "Lifetime prediction for power electronics module substrate mount-down solder interconnect," in *Proc. of International Symposium on High Density Packaging and Microsystem Integration, HDP'07*. IEEE, 2007, pp. 1–10.
- [22] M. Andresen, K. Ma, G. Buticchi, J. Falck, F. Blaabjerg, and M. Liserre, "Junction temperature control for more reliable power electronics," *IEEE Transactions on Power Electronics*, vol. 33, no. 1, pp. 765–776, Jan 2018.
- [23] N. Sintamarean, F. Blaabjerg, H. Wang, F. Iannuzzo, and P. de Place Rimmen, "Reliability oriented design tool for the new generation of grid connected pv-inverters," *IEEE Transactions on Power Electronics*, vol. 30, no. 5, pp. 2635–2644, May 2015.
- [24] K. Ma, R. S. Muñoz-Aguilar, P. Rodríguez, and F. Blaabjerg, "Thermal and efficiency analysis of five-level multilevel-clamped multilevel converter considering grid codes," *IEEE Transactions on Industry Applications*, vol. 50, no. 1, pp. 415–423, Jan 2014.
- [25] A. Wintrich, U. Nicolai, T. Reimann, and W. Tursky, "Application manual power semiconductors." ISLE, 2011.
- [26] M. Andresen, K. Ma, G. D. Carne, G. Buticchi, F. Blaabjerg, and M. Liserre, "Thermal stress analysis of medium-voltage converters for smart transformers," *IEEE Transactions on Power Electronics*, vol. 32, no. 6, pp. 4753–4765, June 2017.

Markus Andresen (S'15-M'17) received the M.Sc. degree in electrical engineering and business administration in 2012 and the Ph.D degree in 2017 from the chair of power electronics at Christian-Albrechts-University of Kiel, Germany. In 2010, he was an intern in the Delta Shanghai Design Center at Delta Electronics (Shanghai) Co., Ltd., China and in 2017 he was a visiting scholar at the University of Wisconsin-Madison, USA. His current research interests include control of power converters and reliability in power electronics. Dr. Andresen was

recipient of one IEEE price paper award on active thermal control of power electronics.

Giovanni De Carne (S'14-M'17) received the M.Sc. in Electrical Engineering from Polytechnic University of Bari, Bari (Italy) in 2013. Since 2013, he carried out his Ph.D. studies at the Chair of Power Electronics at Kiel University, Germany. He defended his doctoral thesis in 2018, and continued working at Kiel university as post-doc on HVDC control and services until 2019. He is currently a Young Scientist at the Institute for Technical Physics at the Karlsruhe Institute of Technology, working on large-scale power hardware in loop systems. He is associate editor of Springer Journal "Electrical Engineering". He is member of PELS, IES and PES, where is an active author and reviewer of journals and conferences of these societies.

Marco Liserre (S'00-M'02-SM'07-F'13) received the MSc and PhD degree in Electrical Engineering from the Bari Polytechnic, respectively in 1998 and 2002. He has been Associate Professor at Bari Polytechnic and from 2012 Professor in reliable power electronics at Aalborg University (Denmark). From 2013 he is Full Professor and he holds the Chair of Power Electronics at Kiel University (Germany). He has published 400 technical papers (more than 1/3 of them in international peer-reviewed journals) and a book. These works have received more than 28000 citations. Marco Liserre is listed in ISI Thomson report "The world's most influential scientific minds" from 2014.

He has been awarded with an ERC Consolidator Grant for the project "The Highly Efficient And Reliable smart Transformer (HEART), a new Heart for the Electric Distribution System". He is member of IAS, PELS, PES and IES. He has been serving all these societies in different capacities. He has received the IES 2009 Early Career Award, the IES 2011 Anthony J. Hornfeck Service Award, the 2014 Dr. Bimal Bose Energy Systems Award, the 2011 Industrial Electronics Magazine best paper award and the Third Prize paper award by the Industrial Power Converter Committee at ECCE 2012, 2012, 2017 IEEE PELS Sustainable Energy Systems Technical Achievement Award and the 2018 IEEE-IES Mittelmann Achievement Award.

Repository KITopen

Dies ist ein Postprint/begutachtetes Manuskript.

Empfohlene Zitierung:

Andresen, M.; De Carne, G.; Liserre, M.

[Load-Dependent Active Thermal Control of Grid-Forming Converters.](#)

2020. IEEE transactions on industry applications, 56

[doi: 10.554/IR/1000118198](#)

Zitierung der Originalveröffentlichung:

Andresen, M.; De Carne, G.; Liserre, M.

[Load-Dependent Active Thermal Control of Grid-Forming Converters.](#)

2020. IEEE transactions on industry applications, 56 (2), 2078–2086.

[doi:10.1109/TIA.2020.2966573](#)

Lizenzinformationen: [KITopen-Lizenz](#)